

# LYAPUNOV-LASALLE BASED DYNAMIC STABILIZATION FOR FIXED WING DRONES

Submitted: 2<sup>nd</sup> March 2022; accepted: 20<sup>th</sup> March 2023

Jean Sawma, Alain Ajami, Thibault Maillot, Joseph el Maalouf

DOI: 10.14313/JAMRIS/4-2023/29

## Abstract:

The market of Unmanned Aerial Vehicles (UAVs) for civil applications is extensively growing. Indeed, these airplanes are now widely used in applications such as data gathering, agriculture monitoring and rescue. The UAVs are required to track a fixed or moving object; thus, tracking control algorithms that ensure the system stability and that have a quick time response must be developed. This paper tackles the problem of supervising a fixed target using a fixed wing UAV flying at a constant altitude and a constant speed. For that purpose, three control algorithms were developed. In all of the algorithms, the UAV is expected to hover around the target in a circular trajectory. Moreover, the three approaches are based upon a Lyapunov-LaSalle stabilization method. The first tracking algorithm ensures that the UAV circles around the target. However, the path that the UAV follows in order to join this pattern is not studied. In the second and third approach, two different techniques that allow the UAV to intercept its final circular pattern in the quickest possible time and thus follow the tangent to the circular pattern are presented. Simulation results that show and compare the performances of the proposed methods are presented.

**Keywords:** UAV, Stabilisation, Lyapunov-LaSalle

## 1. Introduction

Unmanned Aerial Vehicles (UAVs) are now widely used in numerous civil applications including for search and rescue, human or animal surveillance, agriculture and industrial monitoring, firefighting, etc. For these purposes many types of UAV are developed, such as Multi-Rotor drones, Single Rotor Helicopters, fixed wing drones and hybrid VTOL (Vertical Take-Off and Landing). Single and Multi-rotor UAVs benefit from being easy to manufacture, relatively cheap and easy to control. These types of UAVs can take-off and land vertically and can fly with a speed equal to zero. However, they suffer from some disadvantages, in fact, these UAVs are relatively slow (limited speed range), they have limited flying time and range, they are not efficient as they spend a huge amount of energy to fight gravity and finally they have a limited payload. Fixed wing drones are totally different in the sense they benefit from having a long flying time, long range, high efficiency and higher velocity but suffer from being hard to control. Indeed, these airplanes stall at low speed and thus are usually controlled by fixing or minimally varying their linear speed.

Finally, hybrid VTOL combines the benefits of single and multi-rotor UAVs along with fixed wing drones but suffer from being expensive and hard to manufacture.

In almost all UAV applications, the objective is to track a fixed or moving target. This paper focuses on fixed target tracking algorithms using fixed wing UAVs for long range, fixed altitude applications. The drones used in such applications are also called High Altitude Long Endurance (HALE) type UAVs with fixed wings. Since, as mentioned previously, these UAVs could not drop below a minimum linear speed. Thus, the control tracking algorithms applied to these airplanes are challenging. In fact, unlike single and multi-rotor drones, fixed wings UAVs are not capable of reaching and maintaining the target's position. Thus, these drones should follow a specific path in order to track then hover around the target. Consequently, path planning and re-planning based tracking control algorithms are used [8, 14].

The model used in this article is inspired by the Dubins model [12, 24] and [9]. It has been extensively studied for the modeling of vehicles and fixed wing drones, especially in regards to trajectory optimality [2, 7, 18] and [16]. The authors in [1, 4, 22] and [21] provide a review of UAV path planning and re-planning tracking algorithms. In [5] and [3], the problem of dynamic output stabilization of control systems in the unobservable case for fixed wings drones is treated.

The Lyapunov method has been used by several authors, in different ways, such as in [10, 13, 15, 17] and [19]. Lyapunov strategies presented in the literature are not always completely smooth and the final curvature is a bit smaller than the maximum curvature.

In [6, 18] and [23] the authors provided a detailed study of path planning UAV tracking algorithms using Lyapunov-LaSalle based stabilization and time-optimal stabilizing synthesis. The proposed methods have been used to track a circle pattern using a Dubins vehicle.

The paper [18] presents three control algorithms for fixed target tracking using a fixed wing UAV flying at a constant altitude and a constant speed and compares them to a minimum-time path planning algorithm. In order to consider the target reached, the UAV has to maintain a hovering pattern around the target. The proposed tracking algorithms use a circle as a hovering trajectory. This circle has the target as its center. The first tracking algorithm presented herein

is based on a Lyapunov-LaSalle stabilization method and has been studied in [18]. This result is given for the self-consistency of this paper. This method ensures that the UAV is reaching and maintaining the hovering pattern. In the two stabilization methods presented herein, the UAV uses the tangent to the circular pattern as its trajectory guide to get to its destination. The performances of the proposed methods are similar; However, the calculation techniques are different. In fact, the second technique is computed in a new rotating reference frame, while the third one is performed in the stationary reference frame.

The rest of the paper is organized as follows: Section 2 presents the kinematical model of the fixed wings UAV. In Section 3, the presentation of the major results [18] is explored. The first tracking algorithm considered in this paper and the time-optimal synthesis are used as comparison. Section 4 presents the second and third tracking algorithms. Simulation results and algorithms comparison are addressed in Section 5.

## 2. Problem Under Consideration

This section develops the kinematical model of a fixed wing HALE UAV used herein for both simulation and control purposes. The kinematics of a rough HALE drone are supposed to be governed by the standard Dubins equations [11, 24]:

$$\begin{cases} \dot{x} = V_0 \cos(\theta) \\ \dot{y} = V_0 \sin(\theta) \\ \dot{\theta} = u \end{cases} \quad (1)$$

where  $(x, y, \theta) \in \mathbb{R}^2 \times \mathbb{S}^1$  is the state.  $(x, y) \in \mathbb{R}^2$  is the drone's inertial position in a constant altitude plane and  $\theta$  is the yaw angle (the angle made by the aircraft direction with respect to the  $x$ -axis).  $V_0 \in \mathbb{R}^*$  is the linear speed and  $u \in [-u_{max}, u_{max}]$  is the control driving UAV kinematics.

Equation (1) expresses the drones movements in the  $(x, y)$ -plan. The altitude of the UAV is considered constant thus the altitude component is omitted in Eq. (1). Moreover, the speed of the drone  $V_0$  is considered constant. The bound on the yaw angular velocity ( $u$ ) modeled the UAV kinematics restriction on its turning radius, which is given by  $r = \frac{V_0}{u_{max}}$ .

As mentioned previously, in order to track a fixed point (target), the drone has to hover around this target using a circular pattern of radius  $r$ . This final circular pattern is denoted by  $\mathcal{C}$  and has the following characteristics:

- $\mathcal{C}$  center is the target.

- $\mathcal{C}$  radius is  $r = \frac{V_0}{u_{max}}$ .

$\mathcal{C}$  could also be seen as the maximum curvature pattern that can be achieved by the UAV and could be represented by the following equation:

$$\mathcal{C} = \{(x, y, \theta) \mid x = r \sin \theta, y = -r \cos \theta\}. \quad (2)$$

## 3. Lyapunov and Minimal Path Planning

In [18], the authors studied two control strategies for the problem presented previously. The first strategy relies on a Lyapunov-LaSalle stabilization method. The second strategy was constructed using the time-optimal control synthesis for tracking a circle by a Dubins vehicle. In this section, only the principal results of [18] used in this paper are addressed.

### 3.1. Lyapunov-based Strategy

The system modeled with Eq. (1) can be simplified by writing it in a moving-frame. This new frame is sticking to the UAV and thus rotating with it. The system model in the new moving-frame could be calculated by applying the following transformation:

$$\begin{bmatrix} \tilde{x} \\ \tilde{y} \end{bmatrix} = \begin{bmatrix} \cos \theta & \sin \theta \\ -\sin \theta & \cos \theta \end{bmatrix} \begin{bmatrix} x \\ y \end{bmatrix} \quad (3)$$

And thus the system Eq. (1) could be rewritten as:

$$\begin{cases} \dot{\tilde{x}} = u \tilde{y} + V_0 \\ \dot{\tilde{y}} = -u \tilde{x} \end{cases} \quad (4)$$

The system in equation (4) possesses two equilibrium points for  $u = u_{max}$  and  $u = -u_{max}$ , namely  $e_1 = (0, -r)$  and  $e_2 = (0, r)$ . They correspond to the target  $\mathcal{C}$  being circulated counter-clockwise and clockwise, respectively. In the following, the equilibrium point  $e_1$  is the point at the end of the mission where the UAV will hover  $\mathcal{C}$  counter-clockwise. It should be mentioned that point  $e_2$  could also be chosen without modifying the control algorithm performances.

Having chosen  $e_1$  as an equilibrium point, it is possible to switch to a new rotating reference frame  $(\tilde{x}, \tilde{y})$  where the equilibrium point is  $(\tilde{x} = 0, \tilde{y} = 0)$ . The transformation from  $(\tilde{x}, \tilde{y})$  to  $(\bar{x}, \bar{y})$  is given by:

$$\begin{cases} \bar{x} = \tilde{x} \\ \bar{y} = \tilde{y} + r \end{cases} \quad (5)$$

Reaching the equilibrium point  $(\bar{x} = 0, \bar{y} = 0)$  in this new rotating frame is the same as circling the hovering pattern  $\mathcal{C}$  counter-clockwise in the  $(x, y)$ -plane. The system model could be written in the new  $(\bar{x}, \bar{y})$  frame as:

$$\begin{cases} \dot{\bar{x}} = V_0 + u \bar{y} - ru \\ \dot{\bar{y}} = -u \bar{x} \end{cases} \quad (6)$$

The fixed target that the UAV should track is considered to be located at the origin of the  $xy$  fixed reference frame  $(x = 0, y = 0)$ . The UAV starts its tracking mission from an initial position  $(x = x_0, y = y_0)$  and with an initial angle  $(\theta = \theta_0)$  and has to find its path to intercept and maintain a circular hovering pattern that has a radius  $r$  and  $xy$  origin as center. Since the speed of the UAV is constant equal to  $V_0$ , the only parameter that could be modified to meet the control objectives is  $u = \dot{\theta}$ , the UAV angular speed. It should be mentioned that, according to Eq. (1), the input is within the interval  $[-u_{max}, u_{max}]$ .

Knowing this information, let Eq. (7) be a Lyapunov function candidate.

$$V(\bar{x}, \bar{y}) = \bar{x}^2 + \bar{y}^2 \quad (7)$$

After deriving  $V(\bar{x}, \bar{y})$  and combining it with Eq. (6), the following equation is computed:

$$\dot{V}(\bar{x}, \bar{y}) = 2\bar{x}(1 - ru) \quad (8)$$

In order for  $V(\bar{x}, \bar{y})$  to be a Lyapunov function, the following rules should be applied:

- $V(0, 0) = 0$ .
- $V(\bar{x}, \bar{y})$  should be positive.
- $\dot{V}$  should be non-positive.

The first two rules are satisfied. However, to ensure the third one is verified, some conditions on  $u$  are needed. In [18], the authors showed that, if the control  $u$  is equal to a any smooth function  $\bar{K} : \mathbb{R}^2 \rightarrow [-u_{max}, u_{max}]$  that verifies Eq. (9), then  $\dot{V}$  is non-positive.

$$u = \bar{K}(\bar{x}, \bar{y}) = \begin{cases} u_{max} & \text{if } \bar{x} \geq 0 \\ -u_{max} \leq \bar{K}(\bar{x}, \bar{y}) \leq u_{max} & \text{if } \bar{x} < 0 \end{cases} \quad (9)$$

Moreover, according to LaSalle's principle and since  $V$  is a proper function, all the trajectories of system (6) with feedback control  $\bar{K}(\cdot)$  converge to the largest invariant set contained in the set  $E = \{(\bar{x}, \bar{y}) \mid \dot{V}(\bar{x}, \bar{y}) = 0\}$  which has been proved in [18] to be the equilibrium point  $(0, 0)$ . Consequently, there exists an explicit feedback control function  $u(\cdot)$  that has the following propriety: the pattern  $\mathcal{C}$  is a global asymptotically stable attractor for the closed-loop system as a results of applying  $u(\cdot)$ . For example, we may consider the following equation which satisfies (9) and steers asymptotically system (1) to  $\mathcal{C}$ .

$$u = \bar{K}(\bar{x}, \bar{y}) = \begin{cases} a & \text{if } \bar{x} \leq -\epsilon \\ \frac{u_{max}-a}{1+e^{1/(\bar{x}+\epsilon)+1/\bar{x}}} + a & \text{if } \bar{x} \in (-\epsilon, 0) \\ u_{max} & \text{if } \bar{x} \geq 0, \end{cases} \quad (10)$$

where  $\epsilon$  is a positive real number and  $a$  is such that  $-u_{max} \leq a < u_{max}$ .

In other words, the feedback controller (10) turns the UAV with the extremal authorized curvatures ( $u = u_{max}$  or  $u = a$ ) whenever the UAV is moving away from the target ( $\bar{x} \geq 0$  or  $\bar{x} \leq -\epsilon$ ). Thus, the drone will turn until it gets back on track. Whenever the UAV is on track, it will turn with an angular speed equal to  $+a$  hopping to get to its final circular pattern with its minimum turning radius ( $u = u_{max}$ ). The UAV angular speed will vary according to Figure 1 during this approach (when  $\bar{x} \in [-\epsilon, 0]$ ) in order to ensure a smooth transition from  $u = u_{max}$  to  $u = a$  and reduce the chattering effect of this controller. The first tracking control algorithm considered herein is obtained in applying the feedback control defined in Eq. (10).

In order to verify the performances of this controller, the UAV is simulated in closed-loop using MATLAB. The UAV parameters used in numerical simulations are given in Table 1, and the control parameters are  $a = 0.2 \text{ rad/s}$  and  $\epsilon = 10 \text{ m}$ .

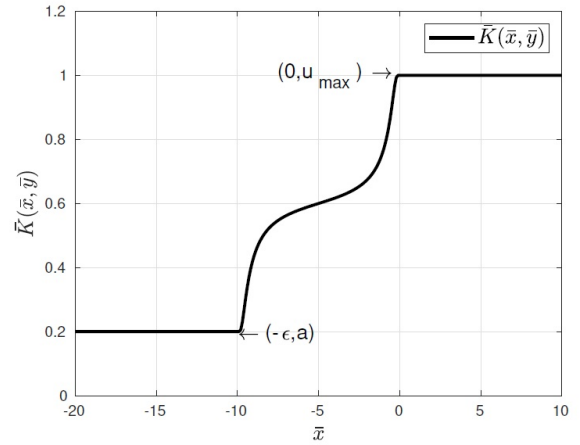


Figure 1. Shape of the feedback controller  $\bar{K}(\bar{x}, \bar{y})$

Table 1. UAV parameters

Description	Symbol	Value	Unit
UAV linear Speed	$V_0$	10	$m/s$
Maximum angular velocity	$u_{max}$	1	$rad/s$
Circular pattern radius	$r$	10	$m$

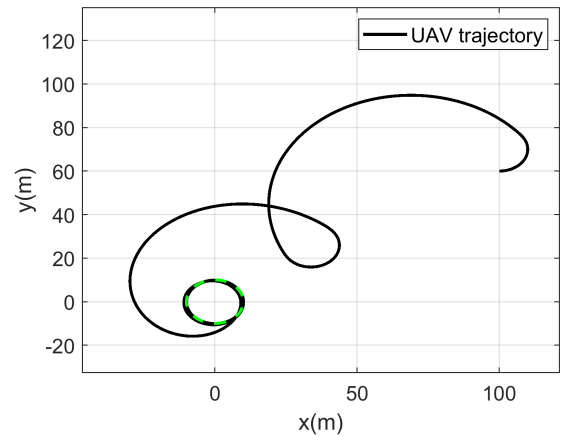


Figure 2. The path followed by the UAV using LaSalle's principle based planification

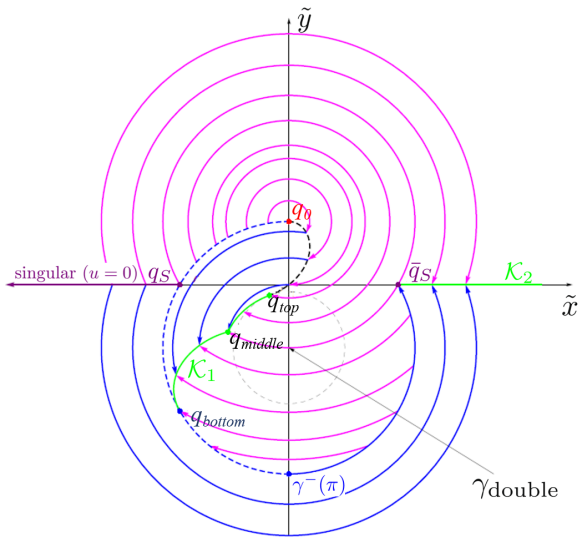
The starting position of the UAV is  $(x_0, y_0, \theta_0)$  equal to  $(100 \text{ m}, 60 \text{ m}, 0 \text{ rad/s})$ .

Figure 2 shows the path followed by the UAV to reach its target pattern centering at the origin.

On this Figure, the path used by the UAV seems to not be time-optimal. Indeed, the UAV is doing loops before reaching and maintaining the final pattern.

### 3.2. Time-optimal Synthesis Based Strategy

Another strategy was presented in [18] in order to find a solution to the problem presented in Section 2. Herein, the minimum time problem for System 1 is addressed, and a summary of this second method based on an time-optimal control synthesis is presented.



**Figure 3.** The optimal synthesis. All optimal trajectories start at  $q_0$  with control  $-1$ . The dashed black curve is the switching curve, the purple curve is the singular trajectory and the green curves are cut loci. Notice that the minimum-time function is not continuous along the blue dashed curve [18].

In order to simplify the treatment up to a dilation in the  $(x, y)$ -plane we may assume without loss of generality that  $V_0 = 1$  and  $[-u_{\max}, u_{\max}] = [-1, 1]$ . Thus, we consider the following problem denoted **(P)**.

**(P)** For every  $(x_0, y_0, \theta_0) \in \mathbb{R}^2 \times S^1$  find the pair trajectory-control joining  $(x_0, y_0, \theta_0)$  to  $\mathcal{C}$ , which is time-optimal for the control system

$$\begin{cases} \dot{x} = \cos \theta \\ \dot{y} = \sin \theta \\ \dot{\theta} = u, \quad u \in [-1, 1]. \end{cases} \quad (11)$$

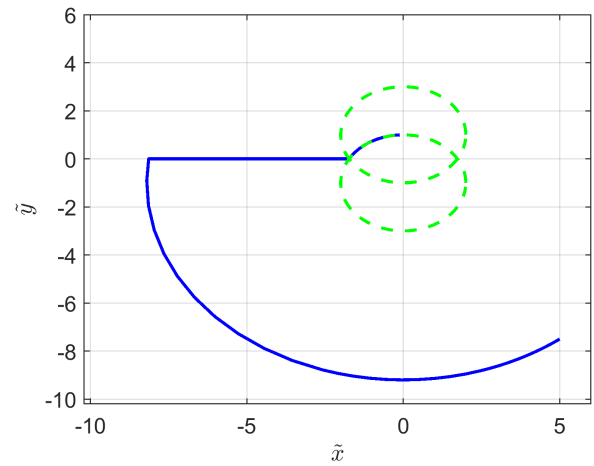
To solve Problem **(P)**, a reduced system in dimension two is computed using Eq. 3: the problem considered is therefore rewritten in the following form denoted **(P')**.

**(P')** For every  $(\tilde{x}_0, \tilde{y}_0) \in \mathbb{R}^2$  find the pair trajectory-control joining  $(\tilde{x}_0, \tilde{y}_0)$  to  $q_0 = (0, 1)$ , which is time-optimal for the control system

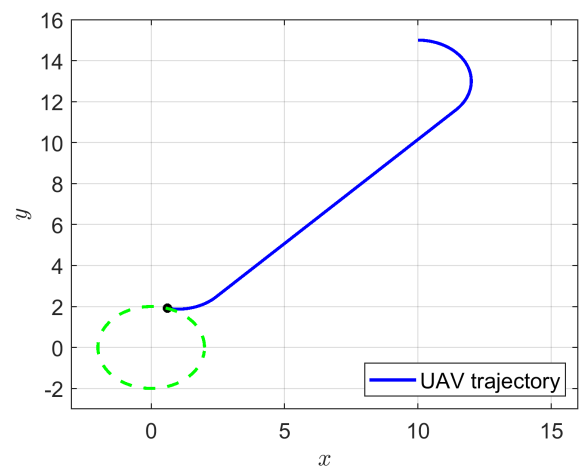
$$\begin{cases} \dot{\tilde{x}} = -u\tilde{y} + 1 \\ \dot{\tilde{y}} = u\tilde{x} \end{cases}, \quad u \in [-1, 1].$$

The time-optimal stabilizing synthesis is the collection of all solution to **(P')** for every  $(\tilde{x}_0, \tilde{y}_0)$  [20]. In [18], authors stated this time-optimal stabilizing synthesis and constructed Figure 3, which is related to the inverse dynamic of the problem. The time-optimal stabilizing synthesis of **(P')** is obtained simply by inverting the arrows of the trajectories represented.

The solutions to problem **(P)** can be deduced from the solutions to problem **(P')**, obtained thanks to the time-optimal stabilizing synthesis represented in Figure 3. Figure 4, shows a pair of plots showing a solution of problem **(P')** (Figure 4a) and its corresponding solution to problem **(P)** (Figure 4b).



(a)



(b)

**Figure 4.** A bang-singular-bang optimal trajectory solution to problem (4a) and the corresponding optimal solution to problem (4b)

## 4. Improvement of the Lyapunov-LaSalle Based Stabilization Method

The objective of this section is to propose two tracking control algorithms that resolve the problem presented in Section 2 with a shorter path than the one obtained with the first Lyapunov-based method stated above. The proposed methods approach the performances of the optimal technique but are computationally less demanding. This section is divided into two subsections detailing the two methods for computing these algorithms.

### 4.1. A First Shorter Stabilization Method

A first technique that allows the fixed wing UAV to slide onto the tangent toward the circular pattern target is detailed in this subsection. It is established in the same way as in Section 3; however, in this controller, the parameter  $a$  used in Eq. (10) is considered a function  $a_2 : \mathbb{R}^{*-} \times \mathbb{R} \rightarrow [-u_{\max}, u_{\max}]$ . Thus, the

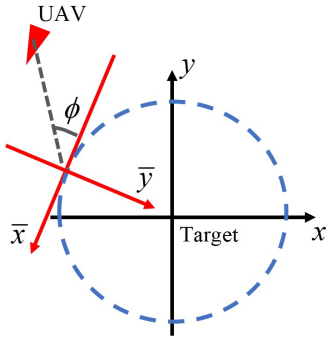


**Figure 5.** The fixed wing UAV in the  $xy$  and  $\bar{x}\bar{y}$  frames

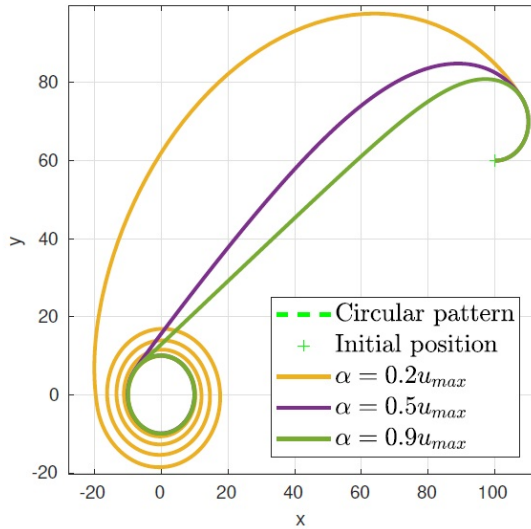


**Figure 6.** The path followed by the UAV to track the target using the minimum time strategy for  $\alpha = 0.2u_{max}$ ,  $\alpha = 0.5u_{max}$  and  $\alpha = 0.9u_{max}$

controller equation (10) is rewritten as follows:

$$u = \bar{K}(\bar{x}, \bar{y}) = \begin{cases} a_2(\bar{x}, \bar{y}) & \text{if } \bar{x} \leq -\epsilon \\ \frac{u_{max} - a_2(\bar{x}, \bar{y})}{1 + e^{1/(\bar{x} + \epsilon) + 1/\bar{x}}} & \text{if } \bar{x} \in (-\epsilon, 0) \\ + a_2(\bar{x}, \bar{y}) & \text{if } \bar{x} \in (-\epsilon, 0) \\ u_{max} & \text{if } \bar{x} \geq 0, \end{cases} \quad (12)$$

Considering  $\bar{x} < 0$ , let  $\phi = \arctan(\bar{y}/\bar{x})$  be the angular coordinate of the UAV in the  $(\bar{x}, \bar{y})$ -plane as represented in Figure 5. Let  $a_2(\bar{x}, \bar{y}) = \alpha \sin(\phi)$  with  $\alpha$  such that  $0 \leq \alpha < u_{max}$ . Thus,  $-u_{max} \leq a_2(\bar{x}, \bar{y}) < u_{max}$ , and the controller defined in Eq. (12) verifies the conditions (9) and stabilizes the system (1) toward the considered pattern as stated in Section 3.

Figure 6 shows the performances of the planning algorithm using the control equation (12) for  $\alpha = 0.2u_{max}$ ,  $\alpha = 0.5u_{max}$  and  $\alpha = 0.9u_{max}$  and  $\epsilon = 10$  m. The UAV starting point is  $(x_0, y_0, \theta_0) = (100$  m,  $60$  m,  $0$  rad/s), and its parameters are given in Table 1. By increasing the value of  $\alpha$ , the time needed to join the pattern is decreased (quicker time response), and by decreasing the value of  $\alpha$ , the UAV

commands have less fluctuation. It should be mentioned that a higher value of  $\alpha$  leads the UAV to slide onto a tangent toward the hovering pattern.

#### 4.2. A Second Simpler Computation Stabilization Method

In this subsection, another method for computing a tracking control algorithm that resolves the problem presented above is established. This algorithm is computed using the stationary coordinates  $(x, y)$  instead of using a rotating reference frame  $(\bar{x}, \bar{y})$ . The stabilization of this system is performed using the same Lyapunov-LaSalle technique as in Section 3. As previously, the parameter  $a$  in Eq. (10) is replaced by a function  $a_3 : \mathbb{R}^2 \rightarrow [-u_{max}, u_{max}]$ . Thus the controller Eq. (10) can be rewritten as:

$$u = \bar{K}(\bar{x}, \bar{y}) = \begin{cases} a_3(\bar{x}, \bar{y}) & \text{if } \bar{x} \leq -\epsilon \\ \frac{u_{max} - a_3(\bar{x}, \bar{y})}{1 + e^{1/(\bar{x} + \epsilon) + 1/\bar{x}}} & \text{if } \bar{x} \in (-\epsilon, 0) \\ + a_3(\bar{x}, \bar{y}) & \text{if } \bar{x} \in (-\epsilon, 0) \\ u_{max} & \text{if } \bar{x} \geq 0, \end{cases} \quad (13)$$

A first step for calculating  $a_3(x, y)$  is to compute the tangent equations of the circular pattern in the  $xy$  stationary frame. Let  $(x_0, y_0)$  be the coordinates of the UAV in the  $xy$  frame. Any line that passes through the UAV has the following equation:

$$y = \ell(x - x_0) + y_0 \quad (14)$$

where  $x, y \in \mathbb{R}$  and  $\ell$  is the slope of the line to be calculated in the following. In order to be a tangent to the circular pattern Equation (14) must also satisfy the circular pattern equation  $(x^2 + y^2 = r^2)$ . Combining both equations leads to the following:

$$a'x^2 + b'x + c' = 0 \quad (15)$$

with

$$\begin{cases} a' = 1 + \ell^2 \\ b' = 2\ell y_0 + 2\ell^2 x_0 \\ c' = y_0^2 + \ell^2 x_0^2 + 2\ell x_0 y_0 - r^2 \end{cases}$$

The solutions of equation (15) are the lines that links the UAV to the circular pattern. Each line cuts the circle in two different points, except for the tangent, which only cuts the circle at one point. Thus, equation (15) double roots can help calculating the tangent equations as follows.

$$\Delta = b'^2 - 4a'c' = a''\ell^2 + b''\ell + c'' = 0 \quad (16)$$

with

$$\begin{cases} a'' = -4x_0^2 + 4r^2 \\ b'' = 8x_0 y_0 \\ c'' = -4y_0^2 + 4r^2 \end{cases}$$

Solving equation (16) results in calculating the two slopes of the two tangents  $\ell_1$  and  $\ell_2$  (Figure 7). It should be mentioned that if no real solution exists, the UAV  $(x_0, y_0)$  is located inside the circular pattern.

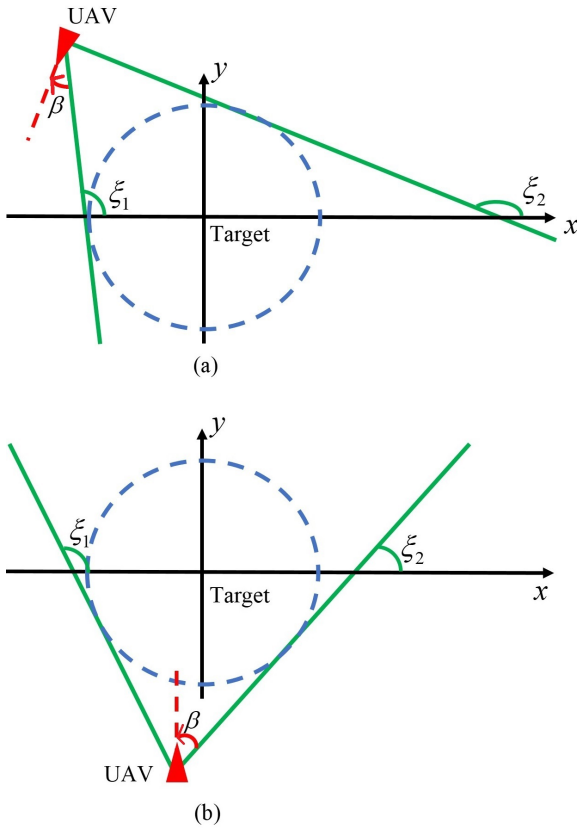


**Figure 7.** Minimum time method in the xy reference frame

Knowing the equations of the two tangents, the UAV should slide on one of them in order to reach its final circular pattern. Indeed, After the computation of the two tangent slopes  $\ell_1$  and  $\ell_2$ , it is possible to calculate the two slope angles  $\xi_1$  and  $\xi_2$  (Figure 7) by applying an arctan function as follows:

$$\xi_{1,2} = \arctan\left(\frac{-8x_0y_0 \pm \sqrt{\Delta'}}{-8x_0^2 + 8r^2}\right) \quad (17)$$

with:

$$\Delta' = b''^2 - 4a''c''$$

In order to have valid slope angles,  $\Delta'$  should be positive or equal to zero which means the following equation should be satisfied:

$$r^2(x_0^2 + y_0^2 - r^2) \geq 0$$

This equation means that the UAV should be outside the hovering pattern.

It should be mentioned that the UAV position  $(x_0, y_0)$  could be written as function of  $\bar{x}$  and  $\bar{y}$  using the following transformation:

$$\begin{aligned} x_0 &= \bar{x} \cos(\theta) - (\bar{y} - r) \sin(\theta) \\ y_0 &= \bar{x} \sin(\theta) + (\bar{y} - r) \cos(\theta) \end{aligned} \quad (18)$$

The tangent that has the lowest value of the slope angle is the one to be chosen since it leads to hovering around the circular pattern counterclockwise. The other tangent with the higher value of the slope

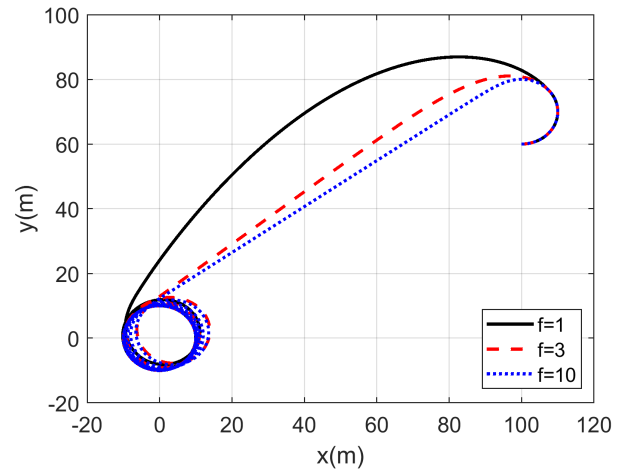


**Figure 8.** The path followed by the UAV for  $f = 1$ ,  $f = 3$  and  $f = 10$  using second tracking algorithm

angle leads to hovering around the circular pattern clockwise. In the following, we will either use  $\xi_1$  or  $\xi_2$  and denoted the chosen angle  $\xi$ .

After computing the angle  $\xi$ , the angle  $\beta = \pi/2 - \xi$  is calculated (Figure 7).  $\beta$  should be within the interval  $[-\pi; \pi]$ . Having  $\beta$ , it is possible to compute  $a_3(x, y)$  as follows:

$$a_3(x, y) = u_{max} \tanh(f\beta) \quad (19)$$

Where  $f > 0$  is a proportional regulation constant. When increasing  $f$ , the time needed in order to converge towards the tangent, will be decreased. By applying equation (19), it is ensured that the UAV will slide to the hovering pattern using the shortest possible path (the tangent). It should be mentioned that  $a_3(x, y)$  satisfies the conditions expressed in Section 3 and ensures the convergence of a controller based on the one given in Equation (10) towards the circular pattern considered.

Finally, the proposed controller algorithm is summarized by the following steps:

- Compute  $\ell_1$  and  $\ell_2$  then  $\xi_1$  and  $\xi_2$
- Choose the tangent that leads to hovering the circular pattern counterclockwise
- Compute  $\beta$
- Compute  $a_3(x, y)$  using equation (19)
- Compute the input to be applied to the UAV (equation (13))

Figure 8 shows the performances of the proposed controller for  $f = 1$ ,  $f = 3$  and  $f = 10$ . The UAV starting point is  $(x_0, y_0, \theta_0)$  equal to (100 m, 60 m, 0 rad/s) and its parameters are given in Table 1,  $\epsilon$  is fixed to 10 m. The results of this method are very similar to the results of the first method conceived in the rotating frame. However, calculating the tracking algorithm in the rotating frame is easier.

### 5. Simulation Results and Comparison

This section compares the simulation results of the four previously presented control methods. The first

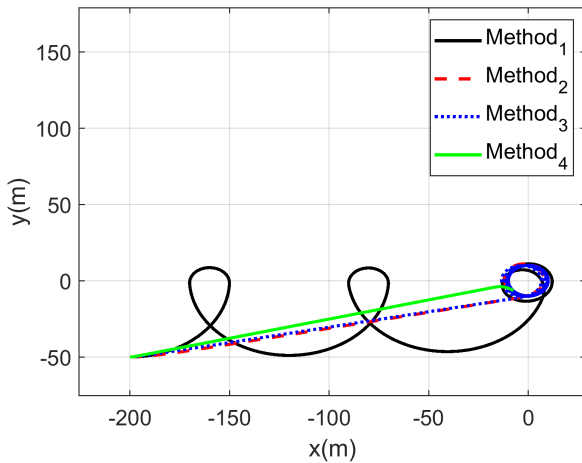


**Figure 9.** The path followed by the UAV using the three proposed algorithms starting from  $(x_0, y_0, \theta_0)$  equal to  $\iota_1 = (-200 \text{ m}, -50 \text{ m}, 0 \text{ rad/s})$

**Table 2.** The time (in seconds) needed by each control algorithm to reach the hovering pattern starting from  $\iota_1$  and  $\iota_2$

	<i>Method</i> <sub>1</sub>	<i>Method</i> <sub>2</sub>	<i>Method</i> <sub>3</sub>	<i>Method</i> <sub>4</sub>
$\iota_1$	43.3s	20.3s	20.3s	19.88s
$\iota_2$	33.0s	13.9s	13.8s	13.38s

control method (*Method*<sub>1</sub>) subject to comparison is the Lyapunov-based method presented in Section 3.1, the second one (*Method*<sub>2</sub>) is the first shorter stabilization method presented in section 4.1, the third one (*Method*<sub>3</sub>) is the second simpler computation stabilization method presented in section 4.2 and the fourth method (*Method*<sub>4</sub>) is the time-optimal method presented in section 3.2.

Multiple initial conditions are considered in order to show the performances of each method. It should be mentioned that the control parameters of the first method are  $a = 0.2 \text{ rad/s}$  and  $\epsilon = 10 \text{ m}$ . The parameters of the second algorithm are  $\alpha = u_{max}$  and  $\epsilon = 10 \text{ m}$ . Finally, the third algorithm parameters are  $f = 10$  and  $\epsilon = 10 \text{ m}$ . The UAV parameters are given in table 1, and the initial conditions  $(x_0, y_0, \theta_0)$  are  $\iota_1 = (-200 \text{ m}, -50 \text{ m}, 0 \text{ rad/s})$  and  $\iota_2 = (50 \text{ m}, -120 \text{ m}, 0 \text{ rad/s})$  respectively.

Figure 9 and 10, show the path followed by the UAV starting from  $(-200 \text{ m}, -50 \text{ m}, 0 \text{ rad/s})$  and  $(50 \text{ m}, -120 \text{ m}, 0 \text{ rad/s})$  respectively, using the proposed tracking control algorithms. The three proposed methods are converging toward the hovering pattern. In the first algorithm (*Method*<sub>1</sub>) the trajectory used to get to the final pattern is twisting. The second and third algorithms (*Method*<sub>2</sub> and *Method*<sub>3</sub>) show trajectories in which the UAV follows the tangent toward the hovering pattern. These three control methods are compared to the time-optimal trajectory (*Method*<sub>4</sub>). Table 2 shows the time needed by the UAV to reach its circular hovering pattern.

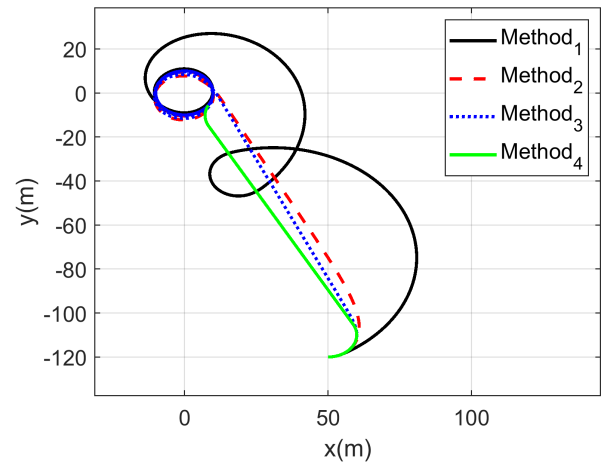


**Figure 10.** The path followed by the UAV using the three proposed algorithms starting from  $(x_0, y_0, \theta_0)$  equal to  $\iota_2 = (50 \text{ m}, -120 \text{ m}, 0 \text{ rad/s})$

*Method*<sub>1</sub> is showing very poor performances compared to *Method*<sub>2</sub>, *Method*<sub>3</sub> and *Method*<sub>4</sub>. Moreover, the optimal method is showing the best possible performances. *Method*<sub>2</sub> and *Method*<sub>3</sub> show very similar performances, despite being calculated in different ways, and their results are very close to *Method*<sub>4</sub>. Finally, it is possible to assume that by carefully choosing parameter  $a(x, y)$  it is possible to obtain nearly time-optimal performances using less computational time.

In summary, the first method employed a computationally efficient algorithm to converge towards the hovering pattern. However, its convergence time was notably slow, making it the least expedient among the four methods presented. The second and third methods have comparable performance, converging towards the circular hovering pattern in nearly optimal time. Both methods were computationally efficient, with the second method being less demanding than the third. The fourth and final algorithm also successfully converged towards the hovering pattern using an optimal trajectory but proved to be computationally demanding.

## 6. Conclusion

This paper studies tracking control algorithms applied to fixed wing UAVs flying at constant speed and constant altitude. Three control algorithms are presented for the tracking of a fixed target. The proposed method ensures the convergence of the UAVs toward a circular hovering pattern.

In the first method, the trajectory obtained did not allow the UAV to reach the pattern quickly. In the second and third method presented above, the trajectories computed follow the direction of the tangent to the pattern, which makes it possible to approach the time-optimal method results.

---

**AUTHORS**

**Jean Sawma\*** – Faculty of Engineering, Saint Joseph University of Beirut, Beirut, Lebanon, e-mail: jean.sawma@usj.edu.lb.

**Alain Ajami** – Faculty of Engineering, Saint Joseph University of Beirut, Beirut, Lebanon, e-mail: alain.ajami@usj.edu.lb.

**Thibault Maillot** – Agrosup, Dijon, France, e-mail: thibault.maillot@agrosupdijon.fr.

**Joseph el Maalouf** – College of Engineering and Technology, American University of the Middle, Kuwait, e-mail: joseph.el-maalouf@aum.edu.kw.

\*Corresponding author

---

**References**

- [1] S. Aggarwal and N. Kumar. "Path planning techniques for unmanned aerial vehicles: A review, solutions, and challenges," *Computer Communications*, vol. 149, 2020, doi: 10.1016/j.comcom.2019.10.014.
- [2] A. Ajami, J.-F. Balmat, J.-P. Gauthier, and T. Maillot. "Path planning and ground control station simulator for UAV," In: *2013 IEEE Aerospace Conference*, 2013, doi: 10.1109/AERO.2013.6496845.
- [3] A. Ajami, M. Brouche, J.-P. Gauthier, and L. Sacchelli. "Output stabilization of military uav in the unobservable case." In: *2020 IEEE Aerospace Conference*, 2020, 1–6, doi: 10.1109/AERO47225.2020.9172770.
- [4] A. Ajami, J.-P. Gauthier, T. Maillot, and U. Serres. "How humans fly," *ESAIM: Control, Optimisation and Calculus of Variations*, vol. 19, no. 4, 2013, 1030–1054.
- [5] A. Ajami, J.-P. Gauthier, and L. Sacchelli. "Dynamic output stabilization of control systems: An unobservable kinematic drone model," *Automatica*, vol. 125, 2021, 109383, doi: 10.1016/j.automatica.2020.109383.
- [6] A. Ajami, J. Sawma, and J. E. Maalouf. "Dynamic stabilization-based trajectory planning for drones," *AIP Conference Proceedings*, vol. 2570, no. 1, 2022, 020003, doi: 10.1063/5.0099757.
- [7] A. Balluchi, A. Bicchi, B. Piccoli, and P. Soueres. "Stability and robustness of optimal synthesis for route tracking by dubins' vehicles." In: *Proceedings of the 39th IEEE Conference on Decision and Control*, vol. 1, 2000, doi: 10.1109/CDC.2000.912827.
- [8] N. Boizot and J.-P. Gauthier. "Motion planning for kinematic systems," *IEEE Transactions on Automatic Control*, vol. 58, no. 6, 2013, 1430–1442, doi: 10.1109/TAC.2012.2232376.
- [9] U. Boscaïn and B. Piccoli. *Optimal Syntheses for Control Systems on 2-D Manifolds*, Springer, 2004.
- [10] D. Campolo, L. Schenato, E. Guglielmelli, and S. S. Sastry. "A Lyapunov-based approach for the control of biomimetic robotic systems with periodic forcing inputs," *IFAC Proceedings Volumes*, vol. 38, no. 1, 2005, 637–641.
- [11] H. Chitsaz and S. M. LaValle. "Time-optimal paths for a dubins airplane." In: *46th IEEE Conference on Decision and Control*, 2007, 2379–2384, doi: 10.1109/CDC.2007.4434966.
- [12] L. E. Dubins. "On curves of minimal length with a constraint on average curvature and with prescribed initial and terminal positions and tangents," *Am. Journ. Math.*, vol. 79, no. 1, 1957, 497–516.
- [13] E. W. Frew, D. A. Lawrence, C. Dixon, J. Elston, and W. J. Pisano. "Lyapunov guidance vector fields for unmanned aircraft applications." In: *2007 American Control Conference*, 2007, 371–376, doi: 10.1109/ACC.2007.4282974.
- [14] J.-P. Gauthier and V. Zakalyukin. "On the motion planning problem, complexity, entropy, and non-holonomic interpolation," *Journal of Dynamical and Control Systems*, vol. 12, no. 3, 2006, 371–404, doi: 10.1007/s10450-006-0005-y.
- [15] M.-D. Hua, T. Hamel, P. Morin, and C. Samson. "A control approach for thrust-propelled underactuated vehicles and its application to vtol drones," *IEEE Transactions on Automatic Control*, vol. 54, no. 8, 2009, 1837–1853, doi: 10.1109/TAC.2009.2024569.
- [16] M.-A. Lagache, U. Serres, and V. Andrieu. "Time minimum synthesis for a kinematic drone model." In: *54th IEEE Conference on Decision and Control (CDC)*, 2015, 4067–4072, doi: 10.1109/CDC.2015.7402852.
- [17] D. A. Lawrence, E. W. Frew, and W. J. Pisano. "Lyapunov vector fields for autonomous unmanned aircraft flight control," *Journal of Guidance, Control, and Dynamics*, vol. 31, no. 5, 2008, 1220–1229, doi: 10.2514/1.34896.
- [18] T. Maillot, U. Boscaïn, J.-P. Gauthier, and U. Serres. "Lyapunov and minimum-time path planning for drones," *Journal of Dynamical and Control Systems*, vol. 21, no. 1, 2015, 47–80, doi: 10.1007/s10883-014-9222-y.
- [19] S. Park, J. Deyst, and J. How. "A new nonlinear guidance logic for trajectory tracking," 2004, doi: 10.2514/6.2004-4900.
- [20] B. Piccoli and H. J. Sussmann. "Regular synthesis and sufficiency conditions for optimality," *SIAM J. Control Optim.*, vol. 39, 1998, 359–410, doi: 10.1137/S0363012999322031.
- [21] Y. Qu, Y. Zhang, and Y. Zhang. "A global path planning algorithm for fixed-wing uavs," *Journal of Intelligent & Robotic Systems*, vol. 91, no. 3, 2018, 691–707, doi: 10.1007/s10846-017-0729-9.

- [22] F. Ropero, P. Muñoz, and M. D. R-Moreno. "Terra: A path planning algorithm for cooperative ugv-uav exploration," *Engineering Applications of Artificial Intelligence*, vol. 78, 2019, 260–272, doi: 10.1016/j.engappai.2018.11.008.
- [23] J. Sawma, A. Ajami, and J. El Maalouf. "Dynamic stability for uav path planning." In: *2022 International Conference on Communications, Information, Electronic and Energy Systems (CIEES)*, 2022, 1–6, doi: 10.1109/CIEES55704.2022.9990803.
- [24] P. Soueres and J.-P. Laumond. "Shortest paths synthesis for a car-like robot," *IEEE Transactions on Automatic Control*, vol. 41, no. 5, 1996, 672–688, doi: 10.1109/9.489204.